1 Back to the ground-state: electron gas

Manfred Lein and Eberhard K. U. Gross

1.1 Introduction

In this chapter, we explore how concepts of time-dependent density functional theory can be useful in the search for more accurate approximations of the *ground-state* exchange-correlation (xc) energy functional.

Within stationary density functional theory, all observables related to the ground-state of an interacting many-electron system can be written as functionals of the ground-state density $n(\boldsymbol{r})$ by virtue of the Hohenberg-Kohn theorem [Hohenberg 1964]. Using the Kohn-Sham approach [Kohn 1965], one considers a non-interacting many-electron system with the same ground-state density as the interacting system. The total energy E of the interacting system is then split into

$$E = T_{\mathrm{KS}} + V_{\mathrm{ext}} + E_{\mathrm{Hxc}} = T_{\mathrm{KS}} + V_{\mathrm{ext}} + E_{\mathrm{H}} + E_{\mathrm{xc}} \,. \tag{1.1}$$

Here T_{KS} is the kinetic energy of the Kohn-Sham system, the second contribution,

$$V_{\mathrm{ext}} = \int \mathrm{d}^3 r \; n(\boldsymbol{r}) v_{\mathrm{ext}}(\boldsymbol{r}) \,, \tag{1.2}$$

is the potential energy due to the external potential $v_{\mathrm{ext}}(\boldsymbol{r})$, and

$$E_{\mathrm{H}} = \frac{1}{2} \int \mathrm{d}^3 r \int \mathrm{d}^3 r' \, \frac{n(\boldsymbol{r}) n(\boldsymbol{r}')}{|\boldsymbol{r} - \boldsymbol{r}'|} \tag{1.3}$$

is the Hartree energy. The xc energy E_{xc} as well as the Hartree-xc energy E_{Hxc} are defined by Eq. (1.1). In the stationary theory, one usually tries to find approximate expressions for the xc energy in terms of the density or the Kohn-Sham orbitals. A different approach is presented in the following. We outline the derivation of the adiabatic-connection fluctuation-dissipation formula which links the ground-state energy to the dynamical response function (cf. [Langreth 1975, Gunnarsson 1976]). We then use TDDFT to relate the correlation energy to the exchange-correlation kernel f_{xc}, and we test the resulting formula by applying it to the uniform electron gas using various approximate exchange-correlation kernels (cf. [Lein 2000b]).

1.2 Adiabatic connection

The principle of adiabatic connection refers to a smooth turning-on of the electron-electron coupling constant λ from zero to unity while keeping the ground-state density fixed, i.e., for each value of λ, the external potential $v_\lambda(\boldsymbol{r})$ is chosen such that the ground-state density of the system with electron-electron interaction $\lambda v_{\mathrm{ee}}(\boldsymbol{r},\boldsymbol{r}') = \lambda/|\boldsymbol{r}-\boldsymbol{r}'|$ equals the ground-state density of the fully interacting system. The Hamiltonian

$$\hat{H}(\lambda) = \hat{T} + \hat{V}(\lambda) + \lambda \hat{V}_{\mathrm{ee}}\,, \tag{1.4}$$

with $\hat{V}(\lambda) = \int \mathrm{d}^3r\, \hat{n}(\boldsymbol{r}) v_\lambda(\boldsymbol{r})$, thus interpolates between the Kohn-Sham Hamiltonian $\hat{H}_{\mathrm{KS}} = \hat{H}(0)$ and the fully interacting Hamiltonian $\hat{H} = \hat{H}(1)$. We first rewrite the Hartree-xc energy as

$$\begin{aligned} E_{\mathrm{Hxc}} &= E - V_{\mathrm{ext}} - T_{\mathrm{KS}} = E - V_{\mathrm{ext}} - E_{\mathrm{KS}} + V_{\mathrm{KS}} \\ &= \int_0^1 \mathrm{d}\lambda\, \frac{\mathrm{d}}{\mathrm{d}\lambda}[E(\lambda) - V(\lambda)]\,. \end{aligned} \tag{1.5}$$

According to the Raleigh-Ritz principle, the ground state $\varPsi(\lambda)$ minimizes the expectation value of $\hat{H}(\lambda)$ so that we have

$$\frac{\mathrm{d}E(\lambda)}{\mathrm{d}\lambda} = \frac{\mathrm{d}}{\mathrm{d}\lambda}\langle \varPsi(\lambda)|\hat{H}(\lambda)|\varPsi(\lambda)\rangle = \langle \varPsi(\lambda)|\frac{\mathrm{d}\hat{H}(\lambda)}{\mathrm{d}\lambda}|\varPsi(\lambda)\rangle\,. \tag{1.6}$$

Similarly, the fact that the density is independent of λ leads to

$$\frac{\mathrm{d}V(\lambda)}{\mathrm{d}\lambda} = \int \mathrm{d}^3r\ n(\boldsymbol{r}) \frac{\mathrm{d}v_\lambda(\boldsymbol{r})}{\mathrm{d}\lambda} = \langle \varPsi(\lambda)|\frac{\mathrm{d}\hat{V}(\lambda)}{\mathrm{d}\lambda}|\varPsi(\lambda)\rangle\,. \tag{1.7}$$

After inserting $\mathrm{d}\hat{H}(\lambda)/\mathrm{d}\lambda = \mathrm{d}\hat{V}(\lambda)/\mathrm{d}\lambda + \hat{V}_{\mathrm{ee}}$ into Eq. (1.6) and substituting Eqs. (1.6) and (1.7) into Eq. (1.5), we arrive at the adiabatic-connection formula

$$E_{\mathrm{Hxc}} = \int_0^1 \mathrm{d}\lambda\ \langle \varPsi(\lambda)|\hat{V}_{\mathrm{ee}}|\varPsi(\lambda)\rangle = \int_0^1 \mathrm{d}\lambda\ V_{\mathrm{ee}}(\lambda)\,. \tag{1.8}$$

Cross Chap.1

To relate this energy to the response function (cf. Section 1.4), we first write the electron-electron interaction

$$\hat{V}_{\mathrm{ee}} = \frac{1}{2}\sum_{j\neq k}^{N} \frac{1}{|\boldsymbol{r}_j - \boldsymbol{r}_k|} = \frac{1}{2}\sum_{j\neq k}^{N} \int \mathrm{d}^3r \int \mathrm{d}^3r'\, \frac{\delta(\boldsymbol{r}-\boldsymbol{r}_j)\,\delta(\boldsymbol{r}'-\boldsymbol{r}_k)}{|\boldsymbol{r}-\boldsymbol{r}'|} \tag{1.9}$$

in terms of the density operator $\hat{n}(\boldsymbol{r}) = \sum_j \delta(\boldsymbol{r}-\boldsymbol{r}_j)$,

$$\hat{V}_{\mathrm{ee}} = \frac{1}{2}\int \mathrm{d}^3r \int \mathrm{d}^3r'\, \frac{1}{|\boldsymbol{r}-\boldsymbol{r}'|}\{\hat{n}(\boldsymbol{r})\hat{n}(\boldsymbol{r}') - \hat{n}(\boldsymbol{r})\delta(\boldsymbol{r}-\boldsymbol{r}')\}\,. \tag{1.10}$$

We then find

$$V_{\mathrm{ee}}(\lambda) = \frac{1}{2}\int \mathrm{d}^3r \int \mathrm{d}^3r' \, \frac{1}{|\boldsymbol{r}-\boldsymbol{r}'|} \times \left\{ \langle \Psi(\lambda)|\hat{n}(\boldsymbol{r})\hat{n}(\boldsymbol{r}')|\Psi(\lambda)\rangle - n(\boldsymbol{r})\delta(\boldsymbol{r}-\boldsymbol{r}') \right\} . \quad (1.11)$$

The expectation value of the product of density operators can be written as

$$\langle \Psi(\lambda)|\hat{n}(\boldsymbol{r})\hat{n}(\boldsymbol{r}')|\Psi(\lambda)\rangle = n(\boldsymbol{r})n(\boldsymbol{r}') + S^{\lambda}(\boldsymbol{r}t,\boldsymbol{r}'t')\big|_{t=t'} , \quad (1.12)$$

where the direct correlation function

$$S^{\lambda}(\boldsymbol{r}t,\boldsymbol{r}'t') = \langle \Psi(\lambda)|\hat{\tilde{n}}(\boldsymbol{r},t)_{\mathrm{H}}\hat{\tilde{n}}(\boldsymbol{r}',t')_{\mathrm{H}}|\Psi(\lambda)\rangle \quad (1.13)$$

characterizes the density fluctuations in the system. Here, $\hat{\tilde{n}}(\boldsymbol{r},t)_{\mathrm{H}} = \hat{n}(\boldsymbol{r},t)_{\mathrm{H}} - n(\boldsymbol{r})$ is the density deviation operator in the Heisenberg picture. The direct correlation function can be expressed in terms of its temporal Fourier transform as

$$S^{\lambda}(\boldsymbol{r}t,\boldsymbol{r}'t') = \int_0^{\infty} \frac{\mathrm{d}\omega}{2\pi} S^{\lambda}(\boldsymbol{r},\boldsymbol{r}',\omega) e^{-i\omega(t-t')} . \quad (1.14)$$

The lower boundary of the integration in Eq. (1.14) has been set to zero because $S^{\lambda}(\boldsymbol{r},\boldsymbol{r}',\omega)$ vanishes for $\omega < 0$. The direct correlation function is related to the response function $\chi^{\lambda}(\boldsymbol{r},\boldsymbol{r}',\omega)$ by the zero-temperature fluctuation-dissipation theorem [Pines 1966],

$$-2\Im\{\chi^{\lambda}(\boldsymbol{r},\boldsymbol{r}',\omega)\} = S^{\lambda}(\boldsymbol{r},\boldsymbol{r}',\omega), \quad \omega > 0 . \quad (1.15)$$

Equation (1.12) can therefore be transformed into

$$\langle \Psi(\lambda)|\hat{n}(\boldsymbol{r})\hat{n}(\boldsymbol{r}')|\Psi(\lambda)\rangle = n(\boldsymbol{r})n(\boldsymbol{r}') - \frac{1}{\pi}\Im \int_0^{\infty} \mathrm{i}\,\mathrm{d}u \; \chi^{\lambda}(\boldsymbol{r},\boldsymbol{r}',\mathrm{i}u) , \quad (1.16)$$

where we have moved the integration path onto the imaginary axis in the complex-frequency plane. For numerical evaluations, the integration over imaginary frequencies is more suitable than the real-frequency integration because it avoids the poles in the response function related to the excitation energies of the system. By combining Eqs. (1.8), (1.11), and (1.16) and exploiting that $\chi^{\lambda}(\boldsymbol{r},\boldsymbol{r}',\mathrm{i}u)$ is real-valued, we obtain the xc energy

$$E_{\mathrm{xc}} = -\frac{1}{2}\int_0^1 \mathrm{d}\lambda \int \mathrm{d}^3r \int \mathrm{d}^3r' \, \frac{1}{|\boldsymbol{r}-\boldsymbol{r}'|} \times \left\{ n(\boldsymbol{r})\delta(\boldsymbol{r}-\boldsymbol{r}') + \frac{1}{\pi}\int_0^{\infty} \mathrm{d}u \; \chi^{\lambda}(\boldsymbol{r},\boldsymbol{r}',\mathrm{i}u) \right\} . \quad (1.17)$$

One can verify by explicit evaluation that the exchange energy is recovered by inserting the response function $\chi_{\mathrm{KS}}(\boldsymbol{r},\boldsymbol{r}',\mathrm{i}u)$ of the non-interacting KS system into Eq. (1.17),

$$E_{\mathrm{x}} = -\frac{1}{2}\int_0^1 \mathrm{d}\lambda \int \mathrm{d}^3r \int \mathrm{d}^3r' \, \frac{1}{|\boldsymbol{r}-\boldsymbol{r}'|} \times \left\{ n(\boldsymbol{r})\delta(\boldsymbol{r}-\boldsymbol{r}') + \frac{1}{\pi}\int_0^\infty \mathrm{d}u \; \chi_{\mathrm{KS}}(\boldsymbol{r},\boldsymbol{r}',\mathrm{i}u) \right\} . \quad (1.18)$$

Comparing Eqs. (1.17) and (1.18), we obtain an expression for the correlation energy,

$$E_{\mathrm{c}} = -\frac{1}{2\pi}\int_0^1 \mathrm{d}\lambda \int \mathrm{d}^3r \int \mathrm{d}^3r' \, \frac{1}{|\boldsymbol{r}-\boldsymbol{r}'|} \times \int_0^\infty \mathrm{d}u \; \left\{ \chi^\lambda(\boldsymbol{r},\boldsymbol{r}',\mathrm{i}u) - \chi_{\mathrm{KS}}(\boldsymbol{r},\boldsymbol{r}',\mathrm{i}u) \right\} . \quad (1.19)$$

Cross Chap. 1

In order to use the last equation for practical calculations, we have to approximate the response function $\chi^\lambda(\boldsymbol{r},\boldsymbol{r}',\mathrm{i}u)$. A possible route to such approximations is provided by the Dyson-type equation (cf. Section 1.4)

$$\chi^\lambda(\boldsymbol{r},\boldsymbol{r}',\omega) - \chi_{\mathrm{KS}}(\boldsymbol{r},\boldsymbol{r}',\omega) = \int \mathrm{d}^3r_1 \int \mathrm{d}^3r_2 \, \chi_{\mathrm{KS}}(\boldsymbol{r},\boldsymbol{r}_1,\omega) \, f^\lambda_{\mathrm{Hxc}}(\boldsymbol{r}_1,\boldsymbol{r}_2,\omega) \, \chi^\lambda(\boldsymbol{r}_2,\boldsymbol{r}',\omega) , \quad (1.20)$$

where

$$f^\lambda_{\mathrm{Hxc}}(\boldsymbol{r}_1,\boldsymbol{r}_2,\omega) = \frac{\lambda}{|\boldsymbol{r}_1-\boldsymbol{r}_2|} + f^\lambda_{\mathrm{xc}}(\boldsymbol{r}_1,\boldsymbol{r}_2,\omega) . \quad (1.21)$$

One way of calculating E_{c} is to approximate χ^λ and f^λ_{xc} independently of each other on the right-hand side of Eq. (1.20) and then substitute into Eq. (1.19). In another approach, one chooses a given approximation for f^λ_{xc} and solves the integral equation (1.20) for χ^λ. The solution of the Dyson-type equation is demanding in general. In the uniform electron gas, however, the translational invariance dictates that the response functions and the xc kernel do not depend independently on two positions but only on the difference between the two coordinates. These quantities can then be expressed in terms of their Fourier transforms:

$$\chi^\lambda(\boldsymbol{r},\boldsymbol{r}',\omega) = \int \frac{\mathrm{d}^3q}{(2\pi)^3} \, \chi^\lambda(q,\omega) e^{i(\boldsymbol{r}-\boldsymbol{r}')\boldsymbol{q}} , \quad (1.22\mathrm{a})$$

$$f^\lambda_{\mathrm{xc}}(\boldsymbol{r},\boldsymbol{r}',\omega) = \int \frac{\mathrm{d}^3q}{(2\pi)^3} \, f^\lambda_{\mathrm{xc}}(q,\omega) e^{i(\boldsymbol{r}-\boldsymbol{r}')\boldsymbol{q}} . \quad (1.22\mathrm{b})$$

The integral in the Dyson equation is then transformed into a simple product, and the solution is found to be

$$\chi^\lambda(q,\omega) = \frac{\chi_{\mathrm{KS}}(q,\omega)}{1 - \chi_{\mathrm{KS}}(q,\omega) f^\lambda_{\mathrm{Hxc}}(q,\omega)} . \quad (1.23)$$

The response function $\chi_{\rm KS}(q,\omega)$ of the non-interacting electron gas is the well-known Lindhard function. At imaginary frequency iu, it is given by [von Barth 1972]

$$\chi_{\rm KS}(q,{\rm i}u) = \frac{k_{\rm F}}{2\pi^2}\left\{\frac{Q^2-\tilde{u}^2-1}{4Q}\ln\frac{\tilde{u}^2+(Q+1)^2}{\tilde{u}^2+(Q-1)^2}\right.$$
$$\left. -1+\tilde{u}\arctan\frac{1+Q}{\tilde{u}}+\tilde{u}\arctan\frac{1-Q}{\tilde{u}}\right\}, \quad (1.24)$$

with

$$Q=\frac{q}{2k_{\rm F}}, \quad \tilde{u}=\frac{u}{qk_{\rm F}}, \quad k_{\rm F}^3=3\pi^2 n\,. \quad (1.25)$$

The correlation energy per electron $\epsilon_{\rm c}$ follows from Eq. (1.19) and Eq. (1.23):

$$\epsilon_{\rm c} = -\frac{1}{\pi^2 n}\int_0^\infty {\rm d}q\int_0^1 {\rm d}\lambda\int_0^\infty {\rm d}u\,\frac{\left[\chi_{\rm KS}(q,{\rm i}u)\right]^2 f^\lambda_{\rm Hxc}(q,{\rm i}u)}{1-\chi_{\rm KS}(q,{\rm i}u)f^\lambda_{\rm Hxc}(q,{\rm i}u)}\,. \quad (1.26)$$

Since the Lindhard function is known, only the xc kernel has to be approximated in Eq. (1.26).

1.3 Scaling properties

In the following, we show that the evaluation of the correlation energy is simplified by a scaling property of the xc kernel: given an approximation for the xc kernel in the fully interacting non-uniform system, the xc kernel for any value of the coupling constant follows immediately.

We are interested in the xc kernel of an interacting system in its ground state. This quantity describes the infinitesimal change of the xc potential due to the influence of a small perturbation. Provided that the time evolution of the slightly perturbed system starts from the ground state, and that we also choose the initial Kohn-Sham state to be the ground state of the Kohn-Sham system, the xc potential can be written as a functional of the time-dependent density only. The xc potential then obeys a scaling relation in the form [Hessler 1999]

$$v^\lambda_{\rm xc}[n](\boldsymbol{r},t) = \lambda^2\, v_{\rm xc}[n'](\lambda\boldsymbol{r},\lambda^2 t)\,, \quad (1.27)$$

with

$$n'(\boldsymbol{r},t) = \lambda^{-3}\, n(\boldsymbol{r}/\lambda, t/\lambda^2)\,. \quad (1.28)$$

A similar relation for the xc kernel follows by taking the functional derivative of Eq. (1.27) with respect to the density:

$$f^\lambda_{\rm xc}[n]\,(\boldsymbol{r}t,\boldsymbol{r}'t') = \lambda^4 f_{\rm xc}[n']\,(\lambda\boldsymbol{r}\;\lambda^2 t, \lambda\boldsymbol{r}'\;\lambda^2 t')\,. \quad (1.29)$$

As we are dealing with the linear-response regime, the xc kernel depends on the difference $(t - t')$ only. Hence we can evaluate the Fourier transform of Eq. (1.29) with respect to $(t - t')$:

$$f_{\mathrm{xc}}^{\lambda}[n]\,(\boldsymbol{r}, \boldsymbol{r}', \omega) = \lambda^2\, f_{\mathrm{xc}}[n']\,(\lambda\boldsymbol{r}, \lambda\boldsymbol{r}', \omega/\lambda^2)\,. \tag{1.30}$$

In the uniform electron gas, the density is constant in space and the xc kernel depends only on the difference $(\boldsymbol{r} - \boldsymbol{r}')$. Then Fourier transformation of Eq. (1.30) with respect to $(\boldsymbol{r} - \boldsymbol{r}')$ yields

$$f_{\mathrm{xc}}^{\lambda}[n]\,(q, \omega) = \lambda^{-1}\, f_{\mathrm{xc}}[n/\lambda^3]\,(q/\lambda,\, \omega/\lambda^2)\,. \tag{1.31}$$

The electron-gas literature often uses the local-field factor $G(q, \omega)$ instead of the xc kernel. At coupling constant λ the two quantities are related by

$$G^{\lambda}(q, \omega) = -\frac{q^2}{4\pi\lambda}\, f_{\mathrm{xc}}^{\lambda}(q, \omega)\,. \tag{1.32}$$

The scaling law for the local-field factor reads

$$G^{\lambda}[n]\,(q, \omega) = G[n/\lambda^3]\,(q/\lambda, \omega/\lambda^2)\,. \tag{1.33}$$

Equation (1.33) shows that the limit $\lambda \to 0$ is closely connected to the high-density limit of $G(q, \omega)$. This becomes even more apparent if we write the local-field factor as a function of the Wigner-Seitz radius r_{s}, the reduced wave vector q/k_{F}, and the reduced frequency $\omega/\omega_{\mathrm{F}}$, with

$$\frac{4\pi}{3} {r_{\mathrm{s}}}^3 = \frac{1}{n}, \quad \omega_{\mathrm{F}} = \frac{k_{\mathrm{F}}^2}{2}\,. \tag{1.34}$$

We then obtain

$$G^{\lambda}(r_{\mathrm{s}}, q/k_{\mathrm{F}}, \omega/\omega_{\mathrm{F}}) = G\,(\lambda r_{\mathrm{s}}, q/k_{\mathrm{F}}, \omega/\omega_{\mathrm{F}})\,. \tag{1.35}$$

1.4 Approximations for the xc kernel

In the uniform electron gas, a number of approximations are available for the xc kernel. Denoting the exact wave-vector dependent and frequency dependent xc kernel of the uniform gas as $f_{\mathrm{xc}}^{\mathrm{hom}}(q, \omega)$, we consider the following approximations:

Random Phase Approximation (RPA) : $f_{\mathrm{xc}}(q, \omega) \equiv 0$.

Adiabatic Local Density Approximation (ALDA) : This is the long-wavelength limit of the static xc kernel:

$$f_{\mathrm{xc}}^{\mathrm{ALDA}}(q, \omega) = \lim_{q \to 0} f_{\mathrm{xc}}^{\mathrm{hom}}(q, 0)\,. \tag{1.36}$$

It can readily be expressed in terms of the xc energy per electron ϵ_{xc}:

$$f_{\mathrm{xc}}^{\mathrm{ALDA}}(q, \omega) = \frac{\mathrm{d}^2}{\mathrm{d}n^2}\left[n \epsilon_{\mathrm{xc}}(n)\right]\,. \tag{1.37}$$

Parametrization by Corradini et al. (see [Corradini 1998]): This approximation for the static xc kernel of the uniform electron gas is a fit to the quantum Monte Carlo data published by Moroni, Ceperley, and Senatore [Moroni 1995]. It satisfies the known asymptotic small-q and large-q limits. Since it interpolates between different values of r_s, it can be evaluated for arbitrary values of the density, in contrast to the original parametrization given in [Moroni 1995].

Parametrization by Richardson and Ashcroft (RA) (see [Richardson 1994]; see also [Lein 2000b] for corrections of typographical errors in the original parametrization): This approximation for the xc kernel at imaginary frequencies is based not upon Monte Carlo data but upon results of numerical calculations by Richardson and Ashcroft. It is constructed to satisfy many known exact conditions. The xc kernel is constructed from Richardson and Ashcroft's local-field factor contributions G_n and G_s via

$$f_{\mathrm{xc}}^{\mathrm{RA}}(q, \mathrm{i}u) = -\frac{4\pi}{q^2}\Big[G_s(Q, \mathrm{i}U) + G_n(Q, \mathrm{i}U)\Big]\,, \tag{1.38}$$

with

$$Q = \frac{q}{2k_\mathrm{F}}, \quad U = \frac{u}{4\omega_\mathrm{F}}\,. \tag{1.39}$$

For the present application, we are fortunate that the RA kernel was derived for imaginary frequencies. Due to its complicated structure near the real axis, the analytic continuation of the xc kernel between imaginary and real axis is not straightforward [Sturm 2000], although it was demonstrated that the continuation of the RA kernel into the complex plane yields good results for the plasmon excitation of the homogeneous electron gas [Tatarczyk 2001]. We also test the static limit of the RA kernel,

$$f_{\mathrm{xc}}^{\mathrm{static\,RA}}(q, \mathrm{i}u) = f_{\mathrm{xc}}^{\mathrm{RA}}(q, 0)\,, \tag{1.40}$$

in order to compare with the static Corradini approximation. (For a comparison of the RA and Monte Carlo f_xc in the static limit, see Fig. 3 of [Moroni 1995].) As a dynamic but spatially local approximation we may use the long-wavelength limit of $f_{\mathrm{xc}}^{\mathrm{RA}}(q, \mathrm{i}u)$,

$$f_{\mathrm{xc}}^{\mathrm{local\,RA}}(q, \mathrm{i}u) = f_{\mathrm{xc}}^{\mathrm{RA}}(0, \mathrm{i}u)\,, \tag{1.41}$$

which we refer to as "local RA".

An approximate xc kernel that is readily applicable to inhomogeneous systems is given by the Petersilka-Gossmann-Gross (PGG) kernel (see [Petersilka 1996a]). This frequency-independent exchange-only approximation was derived in the context of the time-dependent optimized effective potential method [Ullrich 1995a]. Its real-space version reads

$$f_{\mathrm{x}}^{\mathrm{PGG}}(\boldsymbol{r}, \boldsymbol{r}', \omega) = -\frac{2}{|\boldsymbol{r}-\boldsymbol{r}'|}\frac{|\sum_i n_i \varphi_i(\boldsymbol{r})\varphi_i^*(\boldsymbol{r}')|^2}{n(\boldsymbol{r})n(\boldsymbol{r}')}\,, \tag{1.42}$$

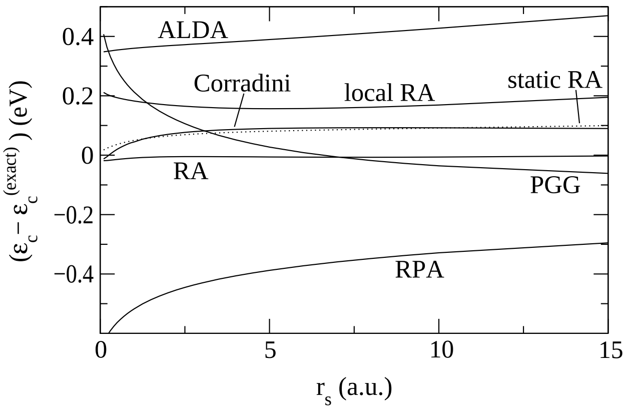

Fig. 1.1. Difference between approximate correlation energies and the exact correlation energy per electron in the uniform electron gas.

where $\varphi_i(\boldsymbol{r})$ and n_i are the ground-state KS orbitals and their occupation numbers (0 or 1). In the uniform gas, transformation to momentum space yields:

$$f_{\mathrm{x}}^{\mathrm{PGG}}(q,\omega) = -\frac{3\pi}{10k_{\mathrm{F}}^2}\left\{\left(\frac{2}{Q}-10Q\right)\ln\frac{1+Q}{|1-Q|}\right.$$
$$\left. + \left(2Q^4-10Q^2\right)\ln\left[(1+\frac{1}{Q})\left|1-\frac{1}{Q}\right|\right] + 11 + 2Q^2\right\}, \qquad (1.43)$$

where $Q = q/(2k_{\mathrm{F}})$. Due to its exchange-only nature, the PGG kernel, taken at coupling constant λ, is simply proportional to λ.

In the following, we evaluate the correlation energy of the uniform electron-gas, Eq. (1.26), for the different xc kernels. We expect that RA's parametrization is close to the exact uniform-gas xc kernel and that the Corradini parametrization is close to the exact static limit. The ALDA is the exact long-wavelength limit of the static xc kernel. Hence, a comparison between these three cases will clarify the importance of both wave-vector and frequency dependence of the xc kernel (for the correlation energy).

Accurate correlation energies are given for example by the parametrization of Perdew and Wang in [Perdew 1992a]. We refer to these values as the "exact" correlation energy $\epsilon_{\mathrm{c}}^{\mathrm{exact}}$. For each choice of xc kernel, the difference between the correlation energy ϵ_{c} and the exact value $\epsilon_{\mathrm{c}}^{\mathrm{exact}}$ is shown in Fig. 1.1 as a function of the density parameter r_{s} in the range $r_{\mathrm{s}} = 0\ldots15$.

The RA results differ by less than 0.02 eV from the exact values, i.e., the RA kernel reproduces the exact correlation energy nearly perfectly. With a deviation of less than 0.1 eV, the Corradini approximation gives a good estimate as well. We note that the result of the *static* version of the RA

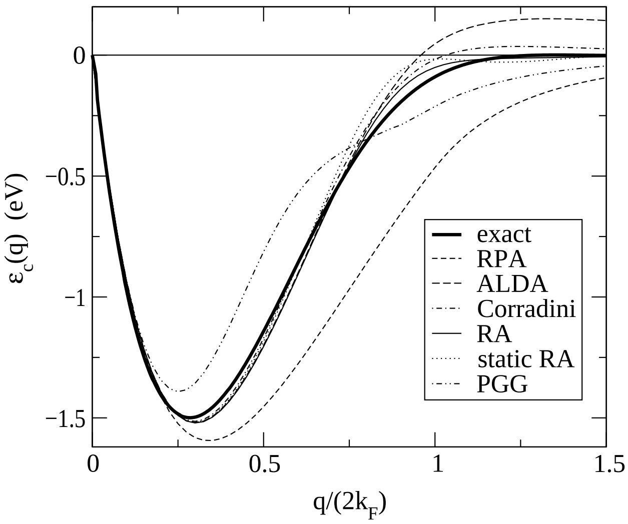

Fig. 1.2. Wave-vector analysis [Eq. (1.44)] of the correlation energy per electron of the uniform gas at $r_s = 4$. Approximations are compared to the "exact" wave-vector analysis of [Perdew 1992b].

formula lies almost on top of the Corradini curve. From this we infer that the small error produced by the Corradini parametrization is in fact due to its static nature. We conclude that neglecting the frequency dependence causes an error typically smaller than 0.1 eV.

It is clearly seen in Fig. 1.1 that the RPA approximation, which neglects the xc kernel completely, makes the correlation energy too negative. The inclusion of the simplest possible choice of kernel, the ALDA kernel, severely over-corrects ϵ_c, so that the absolute deviation from the exact correlation energy remains about the same as in RPA. Furthermore, Fig. 1.1 shows that the local RA (dynamic approximation) performs better than ALDA, but worse than Corradini or static RA. Therefore, it seems that the wave-vector dependence of the xc kernel should be taken into account in order to obtain accurate correlation energies. In other words, the xc kernel is very non-local.

The PGG approximation behaves somewhat differently in that it yields an underestimate of the absolute value of ϵ_c for small r_s and an overestimate for large r_s. It is a very good approximation in the range r_s=5 . . . 10. The behavior near $r_s = 0$ indicates that the PGG kernel differs from the exact exchange-only kernel, since exchange effects should dominate over correlation effects in the high-density limit.

To gain further insight into the effects of the q-dependence and the u-dependence of $f_{xc}(q, iu)$ in Eq. (1.26), we analyze the correlation energy into contributions from density fluctuations of different wave vectors q and imaginary frequencies iu. Equation (1.26) naturally defines a wave-vector analysis

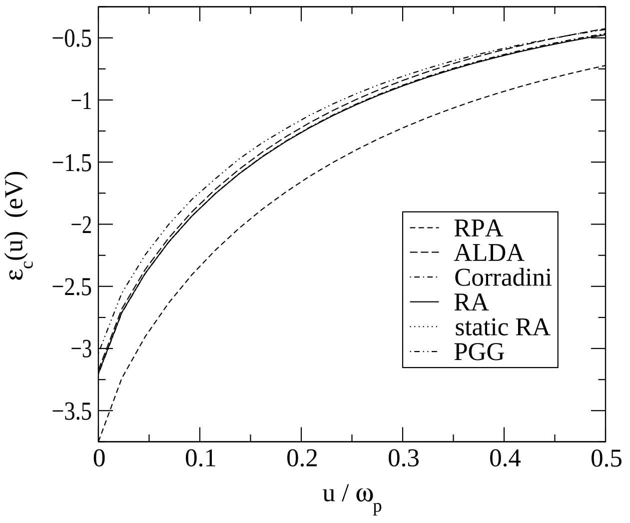

Fig. 1.3. Imaginary-frequency analysis [Eq. (1.47)] of the correlation energy per electron of the uniform gas at $r_\mathrm{s} = 4$ in various approximations (low-frequency regime).

$\epsilon_\mathrm{c}(q)$ if only the q-integration is written explicitly while the other integrations are incorporated in $\epsilon_\mathrm{c}(q)$:

$$\epsilon_\mathrm{c} = \int_0^\infty \mathrm{d}\left(\frac{q}{2k_\mathrm{F}}\right)\epsilon_\mathrm{c}(q)\,. \tag{1.44}$$

The exact wave-vector analysis is essentially given by the Fourier transform of the exact coupling-constant averaged correlation-hole density $n\bar{g}_\mathrm{c}(r)$:

$$\epsilon_\mathrm{c}^\mathrm{exact}(q) = \frac{2k_\mathrm{F}}{\pi} n\bar{g}_\mathrm{c}(q)\,, \tag{1.45}$$

where

$$\bar{g}_\mathrm{c}(q) = \int \mathrm{d}^3r\,\bar{g}_\mathrm{c}(r)\exp(-\mathrm{i}\boldsymbol{qr})\,. \tag{1.46}$$

A parametrization of $\bar{g}_\mathrm{c}(r)$ has been given by Perdew and Wang [Perdew 1992b]. (Although this parametrization misses the non-analytic behavior of $\bar{g}_\mathrm{c}(q)$ at $q{=}2k_\mathrm{F}$, it is otherwise almost “exact”.)

In Fig. 1.2 we compare approximate and “exact” wave-vector analyses for $r_\mathrm{s}{=}4$. While the RPA curve is too negative for all q, we note that ALDA is rather accurate for small q. The ALDA over-correction to ϵ_c comes from positive contributions at large q. To a much smaller extent, the Corradini curve also exhibits this behavior. In general, however, it is close to the exact

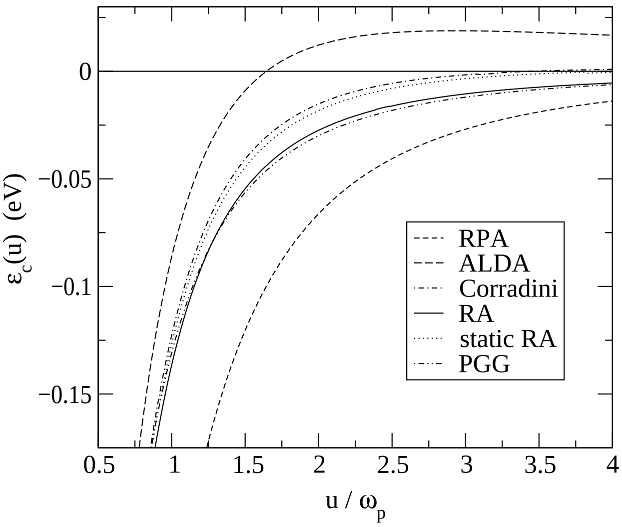

Fig. 1.4. Imaginary-frequency analysis [Eq. (1.47)] of the correlation energy per electron of the uniform gas at $r_s = 4$ in various approximations (high-frequency regime).

wave-vector analysis, as are RA and static RA. In the case of PGG, we note a substantial error cancellation between small and large q-values.

From the last three equations, it is apparent that the large-q behavior of $\epsilon_c(q)$, and therefore $f_{xc}(q, iu)$, is intimately related to the limit of $\bar{g}_c(r)$ at small inter-electron distances r ("on-top" limit). An unphysical divergence for $r \to 0$ is implied by the ALDA kernel and other semilocal approximations as was emphasized by Furche and Van Voorhis [Furche 2005b].

As a complement to the wave-vector analysis, we define the imaginary-frequency analysis $\epsilon_c(u)$ of the correlation energy by writing Eq. (1.26) as an integral over u:

$$\epsilon_c = \int_0^\infty d\left(\frac{u}{\omega_p}\right) \epsilon_c(u) \,, \tag{1.47}$$

with the plasma frequency ω_p given by

$$\omega_p^2 = 4\pi n \,. \tag{1.48}$$

Since $\epsilon_c(u)$ is not known exactly, we must restrict ourselves to a comparison among different approximations, as displayed in Fig. 1.3 (low imaginary frequencies) and Fig. 1.4 (high imaginary frequencies) for r_s=4. In all cases, $\epsilon_c(u)$ starts with a finite negative value at u=0 and then smoothly approaches zero. Assuming that the RA result is the most accurate one, we may assess the performance of the other kernels. Similar to the wave-vector analysis, RPA is too negative over the whole frequency range. For small frequencies, ALDA, Corradini, and RA are practically equal; the differences are located at $u \gtrsim \omega_\mathrm{p}$. In ALDA, $\epsilon_\mathrm{c}(u)$ becomes positive at $u \approx \omega_\mathrm{p}$. PGG exhibits a slight error cancellation between small and high u. Yet, it appears to have a very accurate frequency analysis in the high-u regime. In consistency with the integrated energies, the Corradini curve is very close to the static RA curve. The latter starts to deviate from the dynamic RA at about $u \sim \omega_\mathrm{p}$.

1.5 Concluding remarks

We have seen that the non-locality of the xc kernel, i.e., the non-zero spatial range of $f_\mathrm{xc}(\boldsymbol{r}, \boldsymbol{r}', \omega)$, is essential for the calculation of accurate correlation energies via the adiabatic-connection formula, while the frequency dependence is less important. An analysis of several kernels in the two-dimensional electron gas has been carried out by Asgari et al. [Asgari 2003]. Similar to the three-dimensional case, the frequency dependence was found to be of minor relevance. Contrary to the 3D gas, the over-correction by the ALDA kernel turned out to be less severe.

Recently, the approach based on the fluctuation-dissipation theorem has been applied to a variety of molecules, employing xc kernels derived from standard xc potentials that are used in quantum chemistry [Furche 2005b]. The results indicate that improvement over conventional DFT methods is achieved only with non-local xc kernels.

In analogy to the method described here, one may express the exchange-correlation energy by an adiabatic-connection formula within the framework of time-dependent current-density functional theory [Dion 2005]. This approach still awaits its systematic application to real systems.

While this chapter has focussed on the correlation energy, the next chapter will analyze the xc potentials derived within the adiabatic-connection fluctuation-dissipation framework. Cross Chap. 28

References

Asgari, R., M. Polini, B. Davoudi, and M. P. Tosi, 2003, "Correlation energy of a two-dimensional electron gas from static and dynamic exchange-correlation kernels", *Phys. Rev. B*, vol. 68, pp. 235116-1–6.

Corradini, M., R. Del Sole, G. Onida, and M. Palummo, 1998, "Analytical expressions for the local-field factor $G(\boldsymbol{q})$ and the exchange-correlation kernel $K_{\mathrm{xc}}(\boldsymbol{r})$ of the homogeneous electron gas", *Phys. Rev. B*, vol. 57, pp. 14569–14571.

Dion, M., and K. Burke, 2005, "Coordinate scaling in time-dependent current density functional theory", *Phys. Rev. A*, vol. 72, pp. 020502-1–4(R).

Furche, F., and T. Van Voorhis, T, 2005b, "Fluctuation-dissipation theorem density-functional theory", *J. Chem. Phys.*, vol. 122, pp. 164106–164115.

Gunnarsson, O., and B. I. Lundqvist, 1976, "Exchange and correlation in atoms, molecules, and solids by the spin-density-functional formalism", *Phys. Rev. B*, vol. 13, pp. 4274–4298.

Hessler, P., J. Park, and K. Burke, 1999, "Several Theorems in Time-Dependent Density Functional Theory", *Phys. Rev. Lett.*, vol. 82, pp. 378–381; *ibid* vol. 83, p. 5184(E) (1999).

Hohenberg, P., and W. Kohn, 1964, "Inhomogeneous Electron Gas", *Phys. Rev.*, vol. 136, pp. B864–B871.

Kohn, W., L. J. Sham, 1965, "Self-Consistent Equations Including Exchange and Correlation Effects", *Phys. Rev.*, vol. 140, pp. A1133-A1138.

Langreth, D. C., and J. P. Perdew, 1975, "The exchange-correlation energy of a metallic surface", *Solid State Commun.*, vol. 17, pp. 1425–1429.

Lein, M., E. K. U. Gross, and J. P. Perdew, 2000b, "Electron correlation energies from scaled exchange-correlation kernels: Importance of spatial versus temporal nonlocality", *Phys. Rev. B*, vol. 61, pp. 13431–13437.

Moroni, S., D. M. Ceperley, and G. Senatore, 1995, "Static Response and Local Field Factor of the Electron Gas", *Phys. Rev. Lett.*, vol. 75, pp. 689–692.

Perdew, J. P., and Y. Wang, 1992a, "Accurate and simple analytic representation of the electron-gas correlation energy", *Phys. Rev. B*, vol. 45, pp. 13244–13249.

Perdew, J. P. and Y. Wang, 1992b, "Pair-distribution function and its coupling-constant average for the spin-polarized electron gas", *Phys. Rev. B*, vol. 46, pp. 12947–12954; *ibid*, vol. 56, p. 7018(E) (1997).

Petersilka, M., U. J. Gossmann, and E. K. U. Gross, 1996a, "Excitation Energies from Time-Dependent Density-Functional Theory", *Phys. Rev. Lett.*, vol. 76, pp. 1212–1215.

Pines, D., and P. Nozières, 1966, *The Theory of Quantum Liquids*, vol. 1 (Benjamin, New York).

Richardson, C. F., and N. W. Ashcroft, 1994, "Dynamical local-field factors and effective interactions in the three-dimensional electron liquid", *Phys. Rev. B*, vol. 50, pp. 8170–8181.

Sturm, K., and A. Gusarov, 2000, "Dynamical correlations in the electron gas", *Phys. Rev. B*, vol. 62, pp. 16474–16491.

Tatarczyk, K., A. Schindlmayr, and M. Scheffler, 2001, "Exchange-correlation kernels for excited states in solids", *Phys. Rev. B*, vol. 63, pp. 235106–235112.

Ullrich, C. A., U. J. Gossmann and E. K. U. Gross, 1995a, "Time-dependent optimized effective potential", *Phys. Rev. Lett.*, vol. 74, pp. 872–875.

von Barth, U., and L. Hedin, 1972, "A local exchange-correlation potential for the spin polarized case: I", *J. Phys. C*, vol. 5, pp. 1629–1642.